

Efficient Neural Architecture Search for Emotion Recognition

Monu Verma ^a (monuverma.cv@gmail.com), Murari Mandal ^b,
Satish Kumar Reddy ^c, Yashwanth Reddy Meedimale ^d, Santosh Kumar
Vipparthi^e

^a Electrical and Computer Engineering, University of Miami, Florida, USA,(33146)

^b School of Computer Engineering, Kalinga Institute of Industrial Technology,
Bhubaneswar, Odisha, India, (751024)

^cJP Morgan Chase & Co, Hyderabad, Telangana, India, (500081)

^dWalmart Global Tech, Hyderabad, Telangana, India, (560103)

^eCVPR Lab, Dept. of Electrical Engineering, Indian Institute of Technology, Ropar,
Roopnagar, India (140001)

Corresponding Author:

Santosh Kumar Vipparthi

CVPR Lab, Dept. of Electrical Engineering, Indian Institute of Technology, Ropar,
Roopnagar, India (140001)

Tel: +91-9549658135

Email:skvipparthi@iitrpr.ac.in

Efficient Neural Architecture Search for Emotion Recognition

Monu Verma^a, Murari Mandal^b, Satish Kumar Reddy^c, Yashwanth Reddy Meedimale^d, Santosh Kumar Vipparthi^{e,*}

^a*Electrical and Computer Engineering, University of Miami, Florida, USA, (33146)*

^b*School of Computer Engineering, Kalinga Institute of Industrial Technology, Bhubaneswar, Odisha, India, (751024)*

^c*JP Morgan Chase & Co, Hyderabad, Telangana, India, (500081)*

^d*Walmart Global Tech, Hyderabad, Telangana, India, (560103)*

^e*CVPR Lab, Dept. of Electrical Engineering, Indian Institute of Technology, Ropar, Roopnagar, India (140001)*

Abstract

Automated human emotion recognition from facial expressions is a well-studied problem and still remains a very challenging task. Some efficient or accurate deep learning models have been presented in the literature. However, it is quite difficult to design a model that is both efficient and accurate at the same time. Moreover, identifying the minute feature variations in facial regions for both macro and micro-expressions requires expertise in network design. In this paper, we proposed to search for a highly efficient and robust neural architecture for both macro and micro-level facial expression recognition. To the best of our knowledge, this is the first attempt to design a NAS-based solution for both macro and micro-expression recognition. We produce lightweight models with a gradient-based architecture search algorithm. To maintain consistency between macro and micro-expressions, we utilize dynamic imaging and convert micro-expression sequences into a single frame, preserving the spatiotemporal features in the facial regions. The EmoNAS has evaluated over 13 datasets (7 macro expression datasets: CK+, DISFA, MUG, ISED, OULU-VIS CASIA, FER2013,

*Corresponding author.

Email addresses: monuverma.cv@gmail.com (Monu Verma), murari.mandalfcs@kiit.ac.in (Murari Mandal), mskr181298@gmail.com (Satish Kumar Reddy), yashwanth3130@gmail.com (Yashwanth Reddy Meedimale), skvipparthi@iitrpr.ac.in (Santosh Kumar Vipparthi)

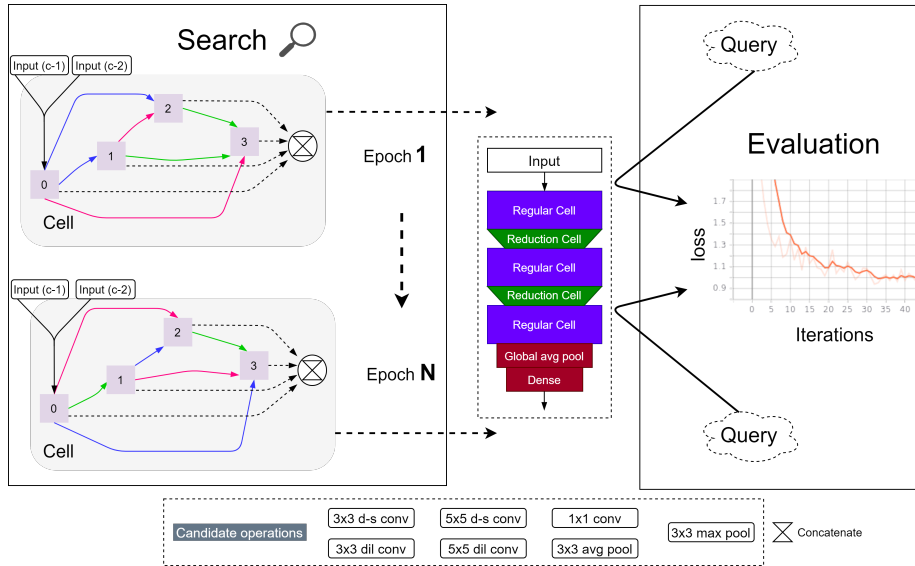


Figure 1: The training and evaluation procedure of the proposed EmoNAS. In the training phase, the regular and reduction cells are optimized. In evaluation, the optimized cells are stacked to classify the input image. *d-s*: *depthwise-separable*, *dil*: *dilated*

RAF-DB, and 6 micro-expression datasets: CASME-I, CASME-II, CAS(ME) $\hat{2}$, SAMM, SMIC, MEGC2019 challenge). The proposed models outperform the existing state-of-the-art methods and perform very well in terms of speed and space complexity.

Keywords: Human emotion, micro-expression, macro-expression, neural architecture search (NAS), deep learning

1. Introduction

Human emotion recognition from visual content has attracted significant attention in the last few decades. Facial appearances are one of the most discriminative features of emotional responses Ekman & Friesen (1971). Therefore, researchers have primarily focused on developing robust facial expression recognition (FER) systems for emotion recognition. It has numerous applications in human-computer interaction, behavior profiling, and smart healthcare solutions.

Facial expressions can be classified into two types: macro and micro-expressions. Macro expressions are considered as a prevailing display of emotions and usually last up to 3 to 4 minutes Ekman (2003). Whereas, micro-expressions are generated when someone tries to hide their actual feelings. Micro-expression appears on the facial region for a fraction of time ($1/3-1/22$) seconds Verma et al. (2019b). The existing state-of-the-art convolutional neural network (CNN) based methods have primarily improved upon the FER performance and few others have focused on improving the efficiency through smaller network design Verma et al. (2019a). However, state-of-the-art approaches require the substantial effort of human expertise to design an effective neural network architecture. Due to the human efforts involved in deep network design, there is room for improvement in both efficiency and accuracy. Moreover, the subtle variations in certain facial regions lead to changes in emotion class. There is a need for developing robust and lightweight FER models for real-world applications.

Recently, there has been a growing interest in developing algorithmic solutions to automatically design an architecture for deep learning models. These algorithms are known as neural architecture search (NAS). Inspired by the differentiable architecture search algorithm Liu et al. (2018b), in this paper, we present EmoNAS to search for the most robust and efficient neural architecture for FER. The training and evaluation procedure of the proposed EmoNAS is shown in Figure 1. As discussed earlier, macro and micro expressions are different in nature, so it is challenging to design a network that can efficiently work for both types of expressions. (more detailed differences between macro and micro expressions are discussed in the supplementary document). Therefore, solutions for both MaEs and MEs are non-identical in the literature. Therefore, Most of the existing FER algorithms are either designed for macro or micro expression classification. Some of the concepts utilize the macro adaptive features for micro-expression classification Sun et al. (2020); Yang et al. (2021). However, there is no single algorithm to solve macro and micro-expression recognition. We made the first attempt to introduce a universal NAS algorithm to solve the generic macro facial expressions as well as micro facial expressions. Usually, a

single instance of an image is sufficient for macro expression recognition analysis whereas, MER requires spatiotemporal data due to its fleeting and short-lived nature. Therefore, to maintain a uniform experimental setting, we adopted the dynamic imaging concept to extract a single instance feature map consisting of the spatiotemporal features from the temporal sequence of frames. Therefore, this paper aims to provide a uniform search and training framework to target the challenges in FER and MER using an EmoNAS. Our proposed framework EmoNAS has the following contributions:

1. We propose a differentiable architecture search-based algorithm named EmoNAS to handle the challenges in macro and micro-expression with the optimized CNN models. We propose to employ a uniform number of cells in the architecture design as used in the search phase. Moreover, the search space is restricted to a shallower structure to obtain lightweight models for real-time applications.
2. The EmoNAS achieves remarkable efficiency improvement over the existing deep learning models in terms of the final model computational complexity.
3. The effectiveness of EmoNAS is validated on 13 datasets: 7 macro facial expression recognition (FER) and 6 micro-expression recognition (MER) datasets. It achieves highly competitive results and outperforms most of all the existing state-of-the-art methods in these 13 datasets. The impact of selecting a different number of cells and nodes is extensively studied by conducting 9 ablation experiments on CK+, DISFSA, CASME-I, and CAS(ME)² datasets.

2. Related Work

2.1. Macro-expression

Macro-expression recognition, commonly referred to as facial expression recognition (FER), has been widely studied in the literature. The deep learning algorithms for FER Pons & Masip (2017); Xie et al. (2020) have far outperformed

the traditional hard-crafted approaches Mandal et al. (2019); Iqbal et al. (2020). Researchers have developed numerous CNN Verma et al. (2019a); Zhang et al. (2016) for FER. Fan et al. Fan et al. (2020) proposed a two-stage attention network to detect posed and spontaneous expressions. Similarly, Li et al. Li et al. (2020b) used attention at the patch and whole-face level for effective FER. Li and Deng Li & Deng (2020) conducted an extensive experiment to delve into the bias across different FER datasets and also explore the intrinsic causes of the dataset discrepancy. Wang et al. Wang et al. (2020b) studied the effect of ambiguous annotations, low-quality expression images, and obscure facial expressions over deep learning networks. A more detailed study of the deep learning-based FER methods is given in Li & Deng (2020).

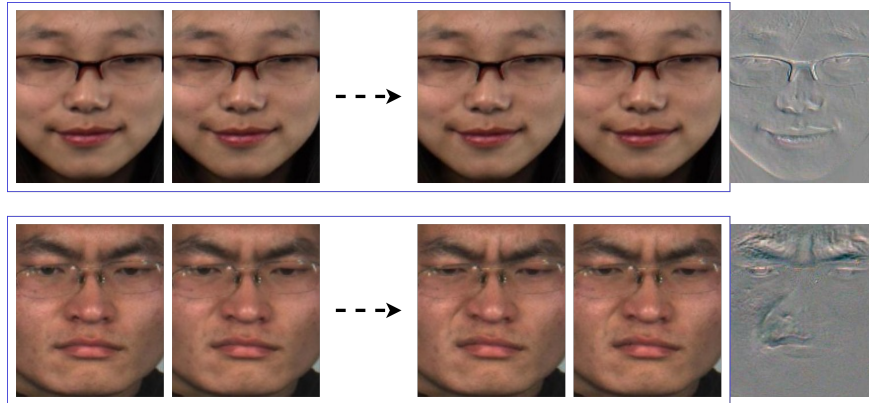
2.2. *Micro-expression*

Micro-expression recognition (MER) has received much attention in past few years. The earlier MER works focused on the spatiotemporal feature descriptors and optical flow Liu et al. (2018c); Xu et al. (2017); Xia et al. (2020). The recent works have used the CNN, RNN, GANs, 3D-CNN and other deep learning techniques to improve the performance Verma et al. (2020b); Sun et al. (2020); Li et al. (2020a); Verma et al. (2020a); Wang et al. (2020a); Van Quang et al. (2019); Liong et al. (2019a). Liong et al. Liong et al. (2019a) proposed a triple stream CNN by using three optical flow features (optical strain, horizontal and vertical optical flow) computed between the onset and apex frames of each sequence. Furthermore, Wang et al. Wang et al. (2020a) proposed an attention-based residual network to guide the CNN towards the micro-expression regions. More recently, a composite database for MER was presented along with the benchmark experimental evaluation protocol in Zhang et al. (2020). Subsequently, Xia et al. Xia et al. (2020) studied the influence of learning complexity on the composite database. They conclude that the low-resolution input and shallower architecture are more suitable for composite-dataset problems in comparison to the deep architectures. A more detailed study of various MER methods can be found in Zhou et al. (2020).

2.3. Neural Architecture Search

Recently NAS algorithms intended for automatically searching and designing CNN architectures have achieved very competitive performance in computer vision tasks such as image classification Real et al. (2019) and object detection Zoph et al. (2018). Despite their remarkable performance, the earlier NAS algorithms were computationally expensive and demands huge memory footprints. The reinforcement learning (RL) Zoph et al. (2018) NAS requires 2000 GPU days to get existing architecture for CIFAR-10 and ImageNet. Similarly, another NAS algorithm Real et al. (2019) needs 3150 GPU days of evaluation. Furthermore, various NAS algorithms Bender et al. (2018); Baker et al. (2017); Liu et al. (2018a) have been introduced to speed up the search process. The RL, evolution, MCTS Negrinho & Gordon (2017), SMBO Liu et al. (2018a) based NAS algorithms consider the architecture search as a black-box optimization problem over a discrete space, which leads to a huge number of architecture assessments. Therefore, Liu et al. (2018b) relaxed the search space to be continuous to optimize the architecture through gradient descent with respect to its validation set performance. This is the most effective solution to accelerate the search process. Therefore, we use this optimization technique in our work. Recently Yu et al. Yu et al. (2020b,a,c) proposed three different NAS based algorithm for facial anti-spoofing. The darts-based approaches have focused on searching the inner cell structure, only. Li et al Li et al. (2021) introduced a NAS-based algorithm Auto-FERNet to automatically search a CNN model on a macro expression dataset.

The network design process for the existing deep learning FER and MER methods requires a lot of manual effort. Usually, the designed network performs well over a few expression datasets but does not transfer well to other expression datasets. Moreover, the macro- and micro-expression recognition tasks require quite different algorithmic approaches to obtain robust performance. Thus, it is difficult to design a single network to effectively solve both the FER and MER tasks. The NAS algorithms offer an alternative approach to universally solving both the FER and MER problems by automatically searching for efficient and



(a) Video sequence (b) Dynamic image

Figure 2: Sample visual representation of the dynamic image response for micro-expression sequences. The dynamic image captures the spatiotemporal features for subtle changes in facial regions.

robust architectures. Motivated by this, we propose the EmoNAS algorithm and experimentally show its effectiveness in FER and MER. To the best of our knowledge, this is the first attempt to solve both macro- and micro-expression tasks with neural architecture search.

3. Dynamic Imaging

The main aim of this paper is to provide a uniform search and training framework to address the challenges in FER and MER using a NAS method. Usually, a single instance of the image is sufficient for FER analysis whereas, MER requires spatiotemporal data due to its fleeting and short-lived nature. Therefore, to maintain a uniform experimental setting, we adopted the dynamic imaging concept to extract a single instance feature map consisting of the spatiotemporal features from the temporal sequence of frames. Most of the existing MER approaches Van Quang et al. (2019); Li et al. (2020a); Liong et al. (2019b); Liu et al. (2019b) rely only on the apex frame for the analysis. However, some studies emphasize the importance of dynamic aspects for detecting the subtle

changes Ambadar et al. (2005) and their effect on the performance of MER. In a micro-expression (MEs) video, each frame has its own significance in the identification of the emotion class. Some recent approaches Reddy Sai Prasanna Teja et al. (2019); Li et al. (2019a) utilized video sequences to design an effective MER system. However, all publicly available MER datasets hold videos with a variant number of frames. In order to normalize the video sequences, some approaches have utilized time interpolation algorithms. This may lose or alter the domain knowledge of micro-expressions by shearing or filling holes in between the frames. To overcome the above-mentioned issues and embed the subtle facial changes, we have utilized the dynamic imaging concept Bilen et al. (2016) to generate a single instance of an image. Dynamic imaging represents the video information into a single instance by conserving high stake active dynamics of MEs. It also ensures uniform search and training architecture for both macro and micro-expression recognition.

The dynamic imaging technique has been effectively used in the recent literature for micro-expression recognition Verma et al. (2019b). The dynamic image interprets the content of the video by aiming at the facial moving regions and compresses that into a single instance. The dynamic image is an RGB response holding the spatiotemporal features of a video sequence. The dynamic image d^* is calculated by Eq. 1-Eq. 5.

$$d^* = \sum_{p=1}^N \mathbb{Z}_p \quad (1)$$

where \mathbb{Z}_p and $N \in q$ represent the p^{th} intermediate motion image and a total number of frames in a video V , respectively. The intermediate motion image is calculated by using Eq. 2.

$$\mathbb{Z}_p = V_p \times F(p) \quad (2)$$

where $F(p)$ implies the frame weight and is calculated by using Eq. 3.

$$F(p) = \sum_{l=p}^q \mathbb{R}(1, l) \quad (3)$$

where $V_p \in V$ represents the p^{th} frame of the video V , $p = 1, 2, \dots, q$ and \mathbb{R} is a ranking function which upgrade the rank of frames as follows:

$$\mathbb{R}(1, l) = \frac{2 \times \mathbb{I}(1, l) - q}{\mathbb{I}(1, l)} \quad (4)$$

$$\mathbb{I}(1, l) = (l, l + 1, l + 2, \dots, q) \quad (5)$$

where q implies the total frames in video sequences. l is a index of the frames in range $[1, q]$. We have shown sample dynamic responses in Figure 2. It can be observed that both the uniform and non-uniform features of a video stream are embedded in a single frame. We use these dynamic images to search and train the NAS models for micro-expression recognition.

4. EmoNAS

The proposed EmoNAS algorithm for architecture search is depicted in Figure 1. We search for a computationally viable cell as the building block of the final architecture. The cell structure is shown in Figure 3. The objective is to discover the optimal cell structure that can lead to the best architecture design for the specific dataset. We use two types of cells: regular cells and reduction cells. Regular cells carry the feature maps to the next cell by maintaining spatial resolution, while reduction cells imply the down-sampling. Further, the learned cell is stacked to form a shallower convolutional network. In the existing method Liu et al. (2018b), the structures discovered through the search process are not necessarily optimal for FER/MER evaluation due to the deep dense final architecture. In literature Verma et al. (2019b); Pasupa & Sunhem (2016), it is well proven that deep networks fail to achieve adequate performance over small-sized datasets. Most of the existing benchmark FER datasets have a lesser number of image/video samples. Also, the features extracted in the search step might get lost or distorted by more cell stacking while training due to repetitive cross-correlation and pooling operations. We are also motivated by the fact that the properties of deep and shallow networks are quite different which has been studied in the literature Srivastava et al. (2015). Therefore, we

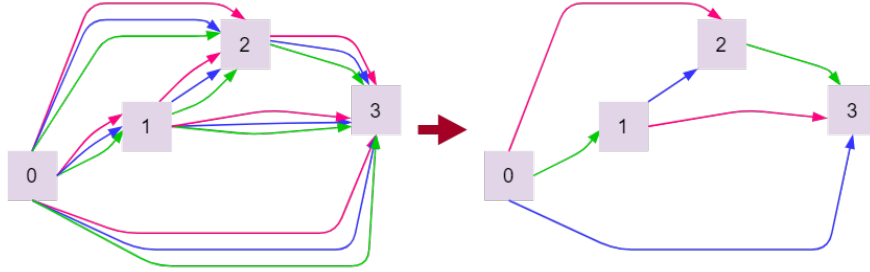


Figure 3: An overview of the cell architecture. Initially, the operations on the edges are unknown. The operations are selected from 7 candidate operations.

stacked search cells (5 cells only) within the premise of shallower networks to ensure better efficiency for real-time applications. Through EmoNAS, we obtain lightweight networks with a minimum number of cells without compromising the quantitative performance.

4.1. Architecture Search Space and Optimization

Our goal is to discover a robust cell topology and use it to develop a convolutional network of cells. A cell is characterized as a directed acyclic graph having N nodes as shown in Figure 3. The nodes represent the feature maps in convolutional networks and the directed edge (m, n) represents an operation $o^{(m,n)}$ that transforms input $x^{(m)}$ into response feature maps. Each cell has 2 input nodes and 1 output node. The cell outputs from the previous layers are used as input nodes. Eventually, the cell structure is formed by learning the set of operations on its edges. A node k in a cell c can be defined by using 5-tuples (P_1, P_2, Q_1, Q_2, S) where, $P_1, P_2 \in \mathbb{P}_k^c$, $Q_1, Q_2 \in \mathbb{Q}$ and S represent selection of input tensors, selection of employed layers over selected input tensors and method used to form an output tensor OT_l^C . Further, the output tensor OT^C of a cell can be calculated by using Eq. 6.

$$OT^C = OT_1^C || OT_2^C || \dots || OT_B^C \quad (6)$$

where $||$ indicate the concatenation operation.

The set of candidate operations are defined by κ , where each operation is denoted by $o(\cdot)$. The continuous search space is used by relaxing the choice of a particular operation to a softmax over all possible operations as given in Eq. 7.

$$\delta^{(m,n)}(x) = \sum_{o \in \kappa} \frac{\exp(\alpha_o^{(m,n)})}{\sum_{o' \in \kappa} \exp(\alpha_{o'}^{(m,n)})} o(x) \quad (7)$$

where the operation mixing weights for a pair of nodes (m, n) are learned by a vector $\alpha^{(m,n)}$ of dimension $|\kappa|$. After the completion of search, a discrete architecture is retrieved by replacing each mixed operation with the most likely operation. We leverage the approximation scheme given in Liu et al. (2018b) to perform the optimization.

Let λ_{train} and λ_{val} represent the training and the validation loss, respectively. These losses are calculated based on both the architecture α and weights w in the network. The goal for EmoNAS is to discover α^* that minimizes the validation loss $\lambda_{val}(w^*, \alpha^*)$. The weights w^* allied with the architecture are computed by minimizing the training loss $w^* = \operatorname{argmin}_w \lambda_{train}(w, \alpha^*)$. Thus, the bilevel optimization problem with α as the upper-level and w as the lower-level variable is represented in Eq. 8 and Eq. 9.

$$\min_{\alpha} \lambda_{val}(w^*(\alpha), \alpha) \quad (8)$$

$$s.t. \quad w^*(\alpha) = \operatorname{argmin}_w \lambda_{train}(w, \alpha) \quad (9)$$

The detailed procedure and approximation technique is outlined in Liu et al. (2018b).

4.2. Network Configurations

The candidate operation space κ consists of the following set of 7 operations: 3×3 depthwise-separable convolution, 5×5 depthwise-separable convolution, identity, 3×3 average pooling, 3×3 max pooling, 3×3 dilated convolution, 5×5 dilated convolution and skip. connection. The network search and evaluation process is discussed below.

4.2.1. Architecture Search

We use 5 cells with each containing 7 nodes. We intentionally select lower number of cells to ensure discovery of lightweight and efficient networks. Similarly, the search space is also limited to only 7 operations. These design decisions helped us to create very lightweight architectures for FER over different datasets. We were also motivated by the success of shallower CNN models in FER to search the shallower architectures through NAS. To compose the nodes in the discrete architecture, we retain the top-2 strongest operations (from distinct nodes) among all the candidate operations. The results analysis discussed in Section 5 validate that search space with 5 cells achieve better performance as compared to DARTS with significant performance improvement over all the FER datasets.

4.2.2. Architecture Evaluation

In order to evaluate the discovered cell, we stack same 5 copies of the cells (searched by architecture search), but untied weights with using either stride 1 or stride 2, as shown in Figure 1 to generate a network. The network is generated by stacking reduction cells at 1/3 and 2/3 locations, the rest of locations are stacked with regular cell in proposed EmoNAS. The number of cells can be adjusted to improve the accuracy/efficiency of the network. We analyze the impact of different parameter changes through ablation study in Section 5.4. Each cell consists of two input nodes and one output node, where input nodes are previous cell outputs and output node is concatenation on all intermediate nodes. At the end of the network, we use global average pooling, followed by a softmax classification layer. Furthermore, we trained the model developed by stacking the cells, on the relevant dataset. More implementation details are presented in Section 5.1.1.

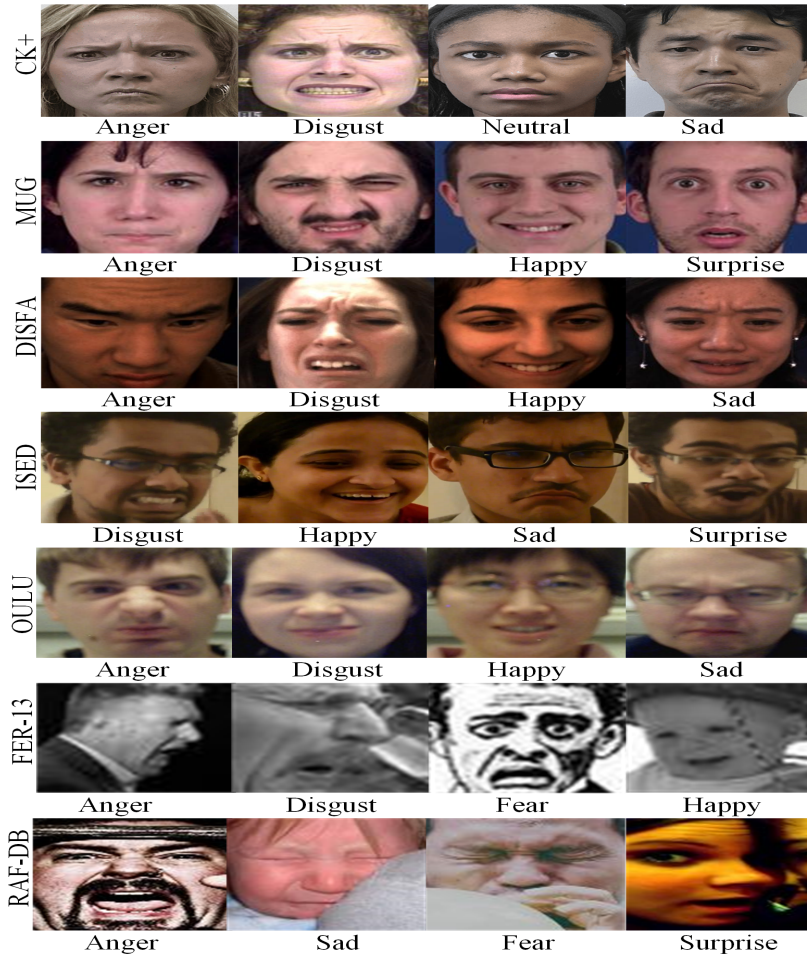


Figure 4: Illustration of different expression samples of macro datasets with challenging tasks a) CK+: posed expressions, b) MUG: posed expressions with enriched resolution, c) DISFA: spontaneous expressions, d) ISED: spontaneous expressions, e) OULU: illumination variations, f) FER-13: Real-time wild expressions, and g) RAF-DB: in-the-wild expressions.

5. Experiments and Results

5.1. Experimental Details

This section discusses the implementation details, dataset, and evaluation strategies. Further, a comparative study of the proposed EmoNAS and state-of-the-art approaches is presented. We carry out the ablation study and com-

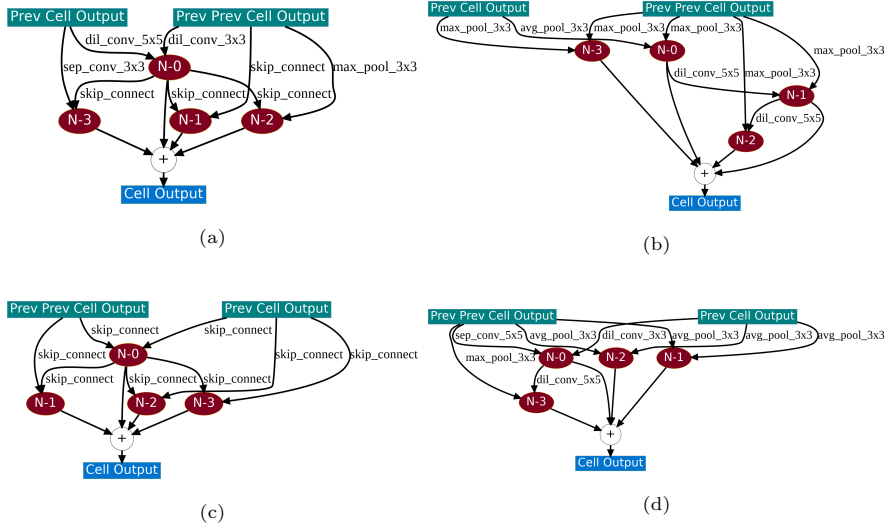


Figure 5: The final regular and reduction cell structures discovered by EmoNAS on (a,b) CK+ (6-Exp), and (c,d) MUG (6-Exp).

putational analysis in the following subsection. document.

5.1.1. Implementation Details

Initially, to search for the best possible cell structure, we used 50 epochs and 16 for batch size due to GPU memory constraints. The main goal of the cell search is to learn the best hyper-parameter α that defines the best possible operations in the cell structure. We used stochastic gradient descent (SGD) optimizer with a momentum of 0.9, a cosine learning rate of 0.007, and a weight decay of $3e^{-4}$. Further, we stacked 5 sets of discovered cells with 7 hidden nodes to design the final EmoNAS architecture. For training a model, similar settings of searching like SGD optimizer with an initial learning rate of 0.007, weight decay $3e^{-4}$, and momentum 0.9 are initialized. The batch size is set to 16, and epochs are set to 70 for training a model. The cross-entropy loss function is used for loss optimization. We implement our model with Pytorch 0.3.1 and run all experiments on an NVIDIA RTX 2080Ti GPU. For each tested dataset, the architecture search is conducted. The same NAS code and hyper-parameters (different image sizes) are used for all the datasets.

<i>Method</i>	<i>Pub-Yr</i>	<i>CK+</i>	
		<i>6 Exp</i>	<i>7 Exp</i>
RADAP Mandal et al. (2019)	IP-19	88.48	83.72
sLSP+LB Iqbal et al. (2020)	TAFF-20	96.77	95.13
VGG16 ¹² Simonyan & Zisserman (2014)	Arxiv-15	91.31	88.18
VGG19 ¹² Simonyan & Zisserman (2014)	Arxiv-15	89.98	78.71
ResNet50 ¹² He et al. (2015)	CVPR-16	89.32	87.31
HiNet Verma et al. (2019a)	LCS-19	91.40	88.60
DCMA-CNN Xie & Hu (2019)	TMM-19	93.46	N/A
DLP-CNN Li et al. (2017)	CVPR-17	95.78	N/A
Lopes Lopes et al. (2017)	PR-17	96.76	95.75
IA-gen Yang et al. (2018)	FG-18	96.57	N/A
Khor-Net Khorrami et al. (2015)	ICCVW-15	95.70	N/A
IF-GAN Cai et al. (2019)	Arxiv-19	95.90	N/A
DARTS * Liu et al. (2018b)	ICML-19	91.50	95.01
P-DART * Chen et al. (2019a)	ICCV-19	85.93	86.85
Auto-FERNet Li et al. (2021)	TNSE-21	N/A	98.89
ViT-SE Aouayeb et al. (2021)	Arxiv-21	N/A	99.80
Squeeze ViT Kim et al. (2022)	Sensors-21	N/A	99.54
EmoNAS	Ours	97.13	96.30

Here, * and $A^a[b]$ implies for re-implemented results and a : results taken from, b : reference of the method. While, *Pub-Yr*, *6 Exp*, and *7 Exp* represent *Publication-Year*, *6 expression*, and *7 expression classes*.

Table 1: Comparative results of the proposed EmoNAS and existing state-of-the-art FER methods on CK+ dataset.

5.1.2. Datasets and Evaluation Settings

To evaluate the proposed EmoNAS, we conduct experiments over 7 macro-expression datasets CK+ Lucey et al. (2010), MUG Aifanti et al. (2010), ISED S. L. Happy et al. (2017), DISFA Mavadati et al. (2013), OULU-CASIA Zhao et al. (2011), FER2013 Kaggle.com (2019 (accessed December 3, 2019), and RAF-DB Li et al. (2017). The sample facial expressions from these datasets are depicted in Figure 4. We adopted a very strict experiment setting of subject/person independent evaluation. The models are tested over completely

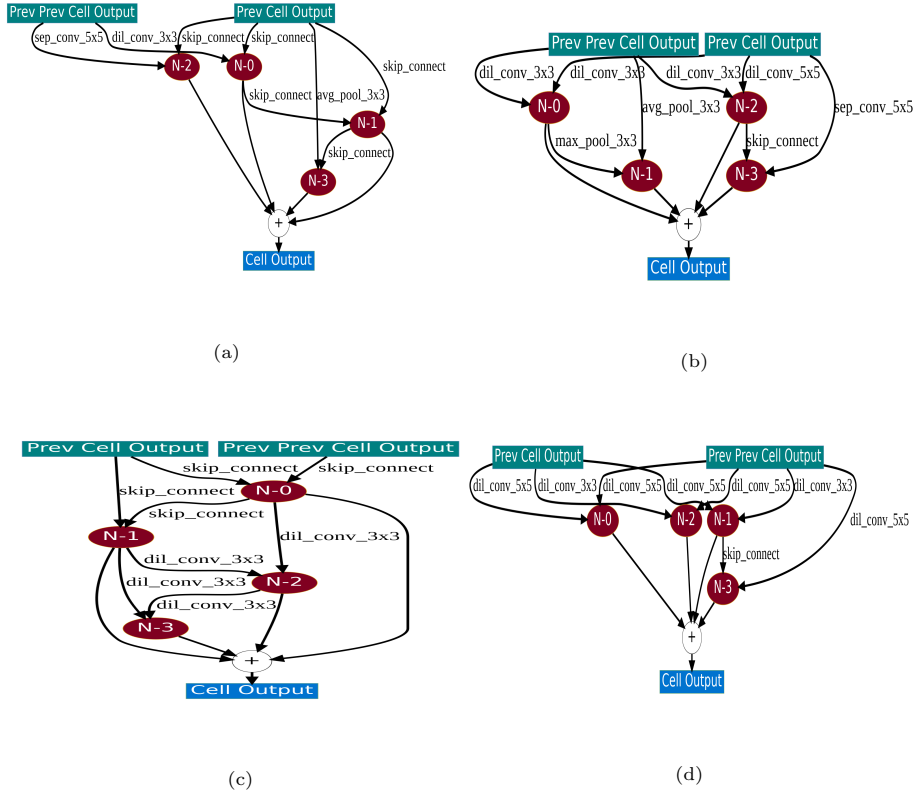


Figure 6: The final regular and reduction cell structures discovered by EmoNAS on (a,b) CASME-II and (c,d) SAMM.

unseen subjects. This makes the achieved results very reliable. For FER2013, we follow the standard train-test scheme presented in the literature Happy & Routray (2017). The input image size of 120×120 is used for CK+, MUG, ISED and DISFA. For OULU-VIS-Strong and FER2013, we use the image size of 128×128 and 48×48 , respectively. The final cell structures discovered by EmoNAS for CK+ (6-exp), MUG (6-exp) are depicted in Figure 5.

We also conduct experiments on 6 micro-expression datasets CASME-I Yan et al. (2013), CASME-II Yan et al. (2014), CAS(ME) 2 Qu et al. (2017), SAMM Davison et al. (2016), SMIC Li et al. (2013), Composite (MEGC2019 challenge) dataset See et al. (2019). The video sequences in these datasets are preprocessed to create dynamic image Bilen et al. (2016). We use input size of 120×120 for

<i>Method</i>	<i>Pub-Yr</i>	<i>MUG</i>		<i>ISED</i>		<i>DISFA</i>	
		<i>6 Exp</i>	<i>7 Exp</i>	<i>4 Exp</i>	<i>5 Exp</i>	<i>6 Exp</i>	<i>7 Exp</i>
RADAP Mandal et al. (2019)	IP-19	82.65	78.57	67.05	N/A	62.38	58.71
sLSP+LB Iqbal et al. (2020)	TAFF-2-	N/A	N/A	78.03	N/A	N/A	N/A
VGG16 ¹² Simonyan & Zisserman (2014)	Arxiv-15	85.14	84.67	73.09	59.32	56.76	57.42
VGG19 ¹² Simonyan & Zisserman (2014)	Arxiv-15	85.22	85.12	70.24	69.20	59.98	53.66
ResNet50 ¹² He et al. (2015)	CVPR-16	86.88	85.58	68.10	63.47	62.48	54.01
HiNet Verma et al. (2019a)	LCS-19	87.80	87.20	N/A	N/A	N/A	N/A
DARTS * Liu et al. (2018b)	ICML-19	94.39	93.70	76.87	47.29	66.55	49.98
P-DART * Chen et al. (2019a)	ICCV-19	67.19	91.16	71.43	53.50	45.14	33.58
EmoNAS	Ours	95.60	96.55	79.93	65.88	69.18	61.2

Table 2: Comparative results of the proposed EmoNAS and existing state-of-the-art FER methods on MUG, ISED, DISFA dataset

all 6 datasets. The final cell structures discovered by EmoNAS for CASME-I, CASME-II, CAS(ME) $\hat{2}$, and SAMM are depicted in Figure 6. Similar to macro-expression, the models are evaluated on completely unseen subjects in leave-one-person-out manner.

5.2. Macro-Expression Results Analysis

We compute the classification accuracy to evaluate the proposed EmoNAS on the macro-expression datasets CK+, MUG, ISED, DISFA, OULO-VIS-Strong, FER2013, and RAF-DB. The results on all the datasets are shown in Table 1, Table 2, Table 3, Table 4, Table 5. The results for VGG16, VGG19, ResNet50 and MobileNet were collected from Mandal et al. (2019) and Verma et al. (2019a).

5.2.1. CK+

The proposed method is compared with existing deep learning methods Xie & Hu (2019); Li et al. (2017); Lopes et al. (2017); Yang et al. (2018); Liu et al. (2014); Khorrani et al. (2015); Cai et al. (2019); Verma et al. (2019a) in Table 1. The architecture discovered by the proposed EmoNAS outperforms the existing state-of-the-art deep learning methods. The proposed NAS-based approach leads to the discovery of lightweight architectures as compared to the existing

FER methods (refer Table 14). From Table 14 we can observe that our model consists of lesser number of parameters (~ 0.55 M) in comparison to manually designed lightweight networks such as MobileNet (~ 3.2 M) and HiNet Verma et al. (2019a) (~ 1 M). In addition, it outperforms the existing methods in quantitative performance as well. EmoNAS obtains 5.73% and 7.7% higher recognition accuracy than HiNet in 6-class and 7-class FER, respectively. Similarly, it also outperforms the existing NAS based method DARTS Liu et al. (2018b) (by 5.63%, 1.29%) and P-DARTS Chen et al. (2019b) (by 11.2%, 9.45%) in 6- and 7-class problems, respectively. The results show that straightforward use of NAS algorithms (designed for generic classification problems) is not sufficient to obtain good performance in FER problems. However, a well-designed NAS method, keeping the challenges in FER in mind, can achieve significantly better performance than the traditional CNN methods. From the results, we can observe that the Auto-FERNet is gaining more accuracy as compared to the proposed EmoNAS for CK+ dataset. However, Auto-FER requires approximately double computational power as compared to the proposed EmoNAS as tabulated in Table 14. Also, recent vision transformer-based models Aouayeb et al. (2021); Kim et al. (2022) are achieving better performance on 7 expression class problems. Still, vision transformer-based models Kim et al. (2022) need a huge computational power than compared to the proposed EmoNAS as reported in Table 14

5.2.2. MUG, ISED and DISFA

We further evaluate the quantitative results for ISED, DISFA, and MUG in Table 2. The MUG consists of posed facial expressions whereas, ISED and DISFA consist of spontaneous expressions. For MUG, the proposed EmoNAS beats the other NAS approaches DARTS Liu et al. (2018b) (by 1.21%, 2.85%) and P-DARTS Chen et al. (2019b) (by 28.41%, 5.39%) in 6- and 7-class FER, respectively. In ISED, our method substantially improves upon the DARTS Liu et al. (2018b) (by 2.76% and 18.59%) and P-DARTS Chen et al. (2019b) (by 8.5% and 12.38%) in 4- and 5-class problems, respectively. Furthermore, in DISFA,

<i>Method</i>	<i>Pub-Yr</i>	<i>OULU-VIS Strong</i>	
		<i>6 Exp</i>	<i>7 Exp</i>
RADAP Mandal et al. (2019)	IP-19	75.83	74.11
VGG16 ¹² Simonyan & Zisserman (2014)	Arxiv-15	73.40	70.70
VGG19 ¹² Simonyan & Zisserman (2014)	Arxiv-15	71.4	70.5
ResNet5 ¹² He et al. (2015)	CVPR-16	73.1	65.4
MobileNet ⁷ Howard et al. (2017)	Arxiv-17	60.9	60.4
HiNet Verma et al. (2019a)	LCS-19	70.3	72.0
EmoNAS	Ours	93.54	90.71

Table 3: Comparative results of the proposed EmoNAS and existing state-of-the-art methods on OULU-VIS Strong dataset

<i>Method</i>	<i>Pub-Yr</i>	<i>7 Exp (pr)</i>
Bag of Words Ionescu et al. (2013)	ICML-13	67.4
Mollahosseini Mollahosseini et al. (2016)	WACV-16	66.4
CNN-Ensemble Liu et al. (2016)	CW-16	65.0
VGG+SVM Georgescu et al. (2018)	IA-18	66.3
GoogleNet Giannopoulos et al. (2018)	AHIM-18	65.2
Fa-Net Wang et al. (2019)	Arxiv-19	62.3
Auto-FERNet Li et al. (2021)	TNSE-21	73.1
EmoNAS	Ours	67.9

Table 4: Comparative results of the proposed EmoNAS and existing state-of-the-art FER methods on FER2013 dataset

the proposed EmoNAS outperforms DARTS Liu et al. (2018b) (by margins of 2.63% and 11.22%) and P-DARTS Chen et al. (2019b) (by margins of 24.04% and 27.62%) in 6- and 7-class problems, respectively. In comparison to the traditional designed CNN networks, the proposed NAS based models show improvement in both the quantitative performance (Table 2) and computational complexity (Table 14). The results also show that the proposed method is effective for both posed and spontaneous FER problems.

<i>Method</i>	<i>Pub-Yr</i>	<i>Angry</i>	<i>Disgust</i>	<i>Fear</i>	<i>Happy</i>	<i>Sad</i>	<i>Surprise</i>	<i>Neutral</i>	<i>Acc.</i>
baseDCNN Li et al. (2017)	CVPR-17	70.99	52.50	50.00	92.91	77.82	79.64	83.09	82.66
Center Loss Li et al. (2017)	CVPR-17	68.52	53.13	54.05	93.08	78.45	79.63	83.24	82.86
DLP-CNN Li et al. (2017)	CVPR-17	71.60	52.15	62.16	92.83	80.13	81.16	80.29	82.74
VGG-FACE Fan et al. (2018)	ICANN-18	82.19	56.62	55.41	86.38	79.52	83.93	71.18	79.16
MRE-VGG Fan et al. (2018)	ICANN-18	83.95	57.50	60.81	88.78	79.92	86.02	80.15	82.63
Kuo et al. Kuo et al. (2018)	CVPRW-18	82.07	44.59	41.25	81.01	44.14	90.12	75.44	72.21
FSN Zhao et al. (2018)	BMVC-18	72.80	46.90	56.80	90.50	81.60	81.80	76.90	81.14
PG-CNN Li et al. (2019b)	TIP-19	-	-	-	-	-	-	-	83.27
SPWFA-SE Li et al. (2020b)	TAFFC-20	-	-	-	-	-	-	-	86.31
DSAN-VGG Fan et al. (2020)	TAFFC-20	82.71	56.25	58.11	94.01	83.89	89.06	80.00	85.37
DSAN-RES Fan et al. (2020)	TAFFC-20	82.10	62.50	55.41	93.00	84.94	79.94	83.97	85.27
ViT-SE Aouayeb et al. (2021)	Arxiv-21	-	-	-	-	-	-	-	87.22
Squeeze ViT Kim et al. (2022)	Sensors-21	-	-	-	-	-	-	-	88.90
DAN Wen et al. (2021)	Arxiv-21	-	-	-	-	-	-	-	85.32
DPOSTER Zheng et al. (2022)	Arxiv-21	-	-	-	-	-	-	-	86.03
EmoNAS	Ours	83.78	86.02	70.62	77.77	83.05	94.85	82.37	87.28

Table 5: Comparative results of the proposed EmoNAS and existing methods on RAF-DB dataset

5.2.3. OULU-VIS-Strong and FER 2013

The quantitative results in OULU-VIS-Strong are shown in Table 3. From Table 3, it is evident that the proposed models derived from EmoNAS obtain superior performance over existing approaches. Our model achieves 23.24%, 18.71% improvement over HiNet in 6- and 7-class FER, respectively. We also evaluate our model over the private test set of FER2013 in the 7-class setting in Table 4. The FER 2013 is a challenging benchmark FER dataset. The previous methods Mollahosseini et al. (2016); Liu et al. (2016); Wang et al. (2019); Giannopoulos et al. (2018); Georgescu et al. (2018); Ionescu et al. (2013) have used the traditional CNN networks to improve the performance. Our NAS-based approach clearly outperforms the existing state-of-the-art approaches Mollahosseini et al. (2016); Liu et al. (2016); Wang et al. (2019); Giannopoulos et al. (2018); Georgescu et al. (2018); Ionescu et al. (2013). This further shows the robustness of the proposed EmoNAS to a variety of FER datasets collected from a diverse set of scenarios.

5.2.4. RAF-DB

We also conduct experiments on the in-the-wild RAF-DB dataset. We search and train the EmoNAS with the seven expression labels provided in the RAF-DB. Table 5 shows the class-wise accuracy and the overall accuracy obtained by EmoNAS for RAF-DB. The class-wise accuracy for anger, disgust, fear, happy, sad, surprise, and neutral (83.78%, 86.02%, 70.62%, 77.77%, 83.05%, 94.85%, 82.37%) show that each specific expression is correctly recognized. We also compare our results with the existing state-of-the-art approaches. The proposed EmoNAS (87.28% overall accuracy) outperforms the all most all other methods in the literature. More specifically, it obtains 2.01%, 1.91%, 0.97%, 4.01% improvement over the recent works published in TIP-19 (PG-CNN Li et al. (2019b)), TAFFC-20 (SPWFA-SE Li et al. (2020b)), TAFFC-20 (DSAN-VGG Fan et al. (2020)), TAFFC-20 (DSAN-RES Fan et al. (2020)), respectively. Furthermore, the results reveal that the EmoNAS attains the highest accuracy when identifying the category of disgust, fear, and surprise. It also maintains good accuracy in the remaining categories, leading to overall accuracy, better than the existing state-of-the-art. Therefore, the features learned and chosen by EmoNAS should contain more discriminative information for FER. This illustrates the effectiveness and superiority of the NAS-based search for the most robust architecture over the traditional CNN models.

5.3. Micro-Expression Results Analysis

Usually, the macro expression recognition algorithms rely on static images for analysis. Whereas, the micro-expression (MEs) recognition algorithms require a video sequence as input. For micro-expression, we use dynamic imaging to generate a single instance of an image micro-expressions. DI ensures uniform search and training architecture for both macro and micro-expression recognition problems. We use the generated dynamic images to search and train the NAS models for micro-expression.

Method	Pub-Yr	Task	CASME-I	CASME-II
MDMO Yong-Jin et al. (2015)	TAFFC-15	[P, N, S, O]	56.29	51.69
SparseMDMO Liu et al. (2018c)	TAFFC-18	[P, N, S, O]	74.83	66.95
CNN-LSTM Wang et al. (2018b)	Neuro-18	[H, S, D, R, O]	60.98	N/A
3D-Flow Li et al. (2019a)	PAA-19	[H, S, D, R, T]	55.44	59.11
Spatio-Temp Kim et al. (2017)	TAFFC-17	[H, S, D, R, O]	N/A	60.98
FuseNet *Reddy Sai Prasanna Teja et al. (2019)	IJCNN-18	[P, N, S, O]	54.84	45.11
3D-ResNet34 * He et al. (2015)	CVPR-16	[P, N, S, O]	55.21	35.21
3D-ResNet50 * He et al. (2015)	CVPR-16	[P, N, S, O]	56.26	35.78
OrigNet Verma et al. (2020b)	IJCNN-20	[P, N, S, O]	66.30	61.58
Aff.Net Verma et al. (2020a)	IEEEEMM-21	[P, N, S, O]	66.99	61.58
DARTS * Liu et al. (2018b)	ICLR-19	[P, N, S, O]	73.72	59.63
P-DART * Chen et al. (2019a)	ICCV-19	[P, N, S, O]	57.03	64.38
AutoMER Verma et al. (2021)	TNNLS-21	[P, N, S, O]	77.58	74.15
ADL_Class	Ablation	[P, N, S, O]	76.04	75.35
EmoNAS	Ours	[P, N, S, O]	80.00	68.42

H: Happy, S: Surprise, D: Disgust, R: Regression, O: Others, P: Positive, N: Negative.

Table 6: Comparative results of the proposed EmoNAS and existing approaches on CASME-I and CASME-II

Method	Pub-Yr	Task	CAS(ME) $\hat{2}$	SAMM
OrigNet Verma et al. (2020b)	IJCNN-20	3/4 EXP	52.85	47.46
Aff.Net Verma et al. (2020a)	IEEEEMM-21	3/4 EXP	54.56	34.89
FuseNet * Reddy Sai Prasanna Teja et al. (2019)	IJCNN-19	3/4 EXP	50.77	46.72
3D-ResNet34 * He et al. (2015)	CVPR-16	3/4 EXP	44.59	47.13
3D-ResNet50 * He et al. (2015)	CVPR-16	3/4 EXP	43.09	49.89
DARTS * Liu et al. (2018b)	ICLR-19	3/4 EXP	58.20	76.98
P-DART * Chen et al. (2019a)	ICCV-19	3/4 EXP	58.19	72.88
AutoMER Verma et al. (2021)	TNNLS-21	3/4 EXP	78.08	72.45
ADL_Class	Ablation	3/4 EXP	70.78	75.11
EmoNAS	Ours	3/4 EXP	71.15	77.04

Table 7: Comparative results of the proposed EmoNAS and existing approaches on CASME $\hat{2}$ and SAMM.

5.3.1. CASME-I and CASME-II

For micro-expression, the effectiveness is examined by testing in terms of average classification accuracy. CASME-I dataset consists of 195 video clips of 35 subjects of Chinese ethnicity. We cataloged the micro-expressions into 4 groups: positive-12, negative-50, surprise-21 and others-106 as given in Verma et al. (2019b). Similarly, CASME-II videos are grouped into positive-12, negative-50, surprise-21, and others-106. Table 6 shows the classification accuracy results for CASME-I and CASME-II. We compare our results with both handcrafted and deep learning methods in the literature. A recently published work in Xia et al. (2020) re-evaluated several previous methods over the leave-one-subject-out (LOSO) protocol for a fair comparison. In our experiments, we follow a similar setup and compare our proposed method with the comparative results as presented in Xia et al. (2020). The proposed EmoNAS significantly outperforms the existing methods in recognition accuracy. It also improves upon the existing NAS methods DARTS Liu et al. (2018b) (by 6.28%, 8.79%) and PDARTS Chen et al. (2019b) (by 22.97%, 4.04%) in CASME-I and CASME-II, respectively.

5.3.2. CAS(ME) $\hat{2}$ and SAMM

CAS(ME) $\hat{2}$ consists of 339 sequences with three emotion classes: anger-101, happy-149, and disgust-88. SAMM includes 159 spontaneous micro-expressions of 29 subjects, recorded at 200 fps. Similar to CASME-I and CASME-II, we combine similar emotion classes to augment 4 groups: positive-27, negative-80, surprise-15, and others-37. Table 7 shows the classification accuracy results for CAS(ME) $\hat{2}$ and SAMM. Our method outperforms the existing methods. More specifically, it outperforms the FuseNet Reddy Sai Prasanna Teja et al. (2019) by 20.38% and 30.32% in CAS(ME) $\hat{2}$ and SAMM, respectively. It also improves upon DARTS Liu et al. (2018b) (by a margin of 12.95% and 0.06%) and PDARTS Chen et al. (2019b) (by a margin of 12.96% and 4.16%) in CAS(ME) $\hat{2}$ and SAMM, respectively.

<i>Method</i>	<i>Pub-Year</i>	<i>SMIC</i>		<i>COMPOSITE</i>
		<i>Acc.</i>	<i>UAR</i>	<i>UAR</i>
LBP-TOP Guoying & Pietikainen (2007)	A-Tran-07	N/A	52.80	57.85
MDMO Yong-Jin et al. (2015)	TAFFC-15	64.00	56.91	N/A
OffApexNet Gan et al. (2019)	SP-IC-19	67.68	N/A	N/A
CNN-LSTM Wang et al. (2018a)	Ar-18	N/A	41.25	39.24
TSCNN Song et al. (2019)	Access-19	N/A	54.12	59.48
STSTNet Liong et al. (2019a)	FG-19	N/A	59.95	67.24
NMER Liu et al. (2019b)	FG-19	N/A	55.55	59.36
DualInc Zhou et al. (2019)	FG-19	N/A	61.49	68.58
CapsuleNet Van Quang et al. (2019)	FG-19	N/A	58.77	65.06
DCN-DB Xia et al. (2019)	ICBEA-19	N/A	59.79	60.37
DSSN Khor et al. (2019)	ICIP-19	63.41	N/A	N/A
RCN-W Xia et al. (2020)	TIP-20	N/A	66.00	71.00
LGCconD Li et al. (2020a)	TIP-20	63.41	N/A	N/A
AutoMER Verma et al. (2021)	TNNLS	81.20	N/A	N/A
ADL_Class	Ablation	71.39	58.54	78.76
EmoNAS	Ours	77.09	69.03	73.22

Table 8: Recognition accuracy and unweighted average recall (UAR) comparison on SMIC and Composite dataset (MEGC2019 Challenge)

<i>#Cells</i>	<i>#Nodes</i>		
	6	7	8
5	95.67	97.13	95.96
8	84.93	85.23	83.88
10	96.15	96.04	95.84
15	94.78	96.11	93.42

Table 9: EmoNAS ablation analysis on CK+ with 6 expressions

5.3.3. SMIC and Composite Dataset

We also conduct experiments on SMIC and the Composite dataset See et al. (2019). SMIC consists of 164 emotion sequences from 16 subjects. The emotions are grouped into positive-51, negative-70, and surprise-43. The Composite dataset is collected by combining three emotion classes (negative, positive, and

<i>#Cells</i>	<i>#Nodes</i>		
	6	7	8
5	63.89	69.18	72.57
8	68.84	73.28	71.54
10	64.63	69.89	73.37
15	65.68	67.17	71.03

Table 10: EmoNAS ablation analysis on DISFA with 6 expressions

surprise) of three datasets CASME-II, SAMM, and SMIC as given in MEGC-2019 See et al. (2019) challenge. The quantitative results for SMIC and Composite datasets are given in Table 8. In SMIC, the proposed EmoNAS obtains superior recognition accuracy and unweighted average recall (UAR) over the existing methods. It outperforms the most recent method LGCconD Li et al. (2020a) (TIP-20) in accuracy by a margin of 13.68%. Similarly, it outperforms RCN-W Xia et al. (2020) (TIP-20) in UAR by 3.03% margin. In the Composite dataset, our EmoNAS achieves 2.22% higher UAR as compared to the current state-of-the-art method RCN-W Xia et al. (2020) (TIP-20).

5.4. Ablation Study

We study the effect of multiple components of EmoNAS through ablation analysis to understand its behavior for the task of FER. We conduct experiments on two macro-expression datasets CK+, DISFA, and two micro-expression datasets. The ablation results are shown in Table 9, Table 10, Table 11, and Table 12. We change the number of nodes within each cell to 6, 7, and 8 nodes. We stack these cells with 5, 8, 10, and 15 repetitions to obtain 12 different CNN structures. Thus, for each dataset, we conduct 12 ablation experiments.

From Table 9 and Table 10 we can see that increasing the number nodes to 8 or decreasing to 6 resulted in marginal decrease or increase in the accuracy for CK+ and DISFA. Similarly, increasing the number of cells to 10/15 doesn't improve the performance substantially in both datasets. Moreover, a higher number of cells would increase the network complexity. Therefore, in most

<i>#Cells</i>	<i>#Nodes</i>		
	6	7	8
5	69.50	80.00	70.65
8	79.29	74.31	73.46
10	73.37	77.19	76.17
15	75.74	72.11	74.52

Table 11: EmoNAS ablation analysis on CASME-I

<i>#Cells</i>	<i>#Nodes</i>		
	6	7	8
5	67.90	71.15	69.30
8	73.25	74.95	69.82
10	70.44	67.57	62.16
15	70.63	65.56	60.56

Table 12: EmoNAS ablation analysis on CAS(ME) $\hat{2}$

cases, we select 5 cells with each having 7 nodes to maintain a good trade-off between accuracy and model efficiency. The micro-expression ablations results are given in Table 11 and Table 12. The best performance is achieved with 5 cells and 7 nodes. This again shows that the combination of 5 cells and 7 nodes are the most suitable parameters for FER datasets. These results also prove the literature Verma et al. (2019b); Pasupa & Sunhem (2016); Srivastava et al. (2015) deep networks fail to achieve adequate performance over small-sized datasets. In addition, we conducted an ablation study with the architecture search of the autodeeplab Liu et al. (2019a) for the classification (ADL_Class). The experiments are conducted over the five micro expression datasets CASME-I, CASME-II, CAS(ME) $\hat{2}$, SMIC, SAMM along with Composite dataset and the results are included in Table 6, 7 and 8.

Dataset	Input Size	Size(mb)	Speed(fps)	Params(M)
CK+	120 × 120	15.45	60.30	0.90
MUG	120 × 120	13.75	17.15	0.49
ISED	120 × 120	13.93	56.25	0.51
DISFA	120 × 120	14.15	30.90	0.58
OULU-VIS-Strong	128 × 128	14.00	54.50	0.59
FER2013	48 × 48	7.43	200.80	1.36
CASME-I	128 × 128	14.63	42.45	0.70
CASME-II	180 × 180	16.43	32.63	0.82
CAS(ME) $\hat{2}$	180 × 180	14.94	31.68	0.53
SAMM	120 × 120	13.64	40.56	0.6

Table 13: Memory, speed, and complexity analysis of EmoNAS models discovered on macro: CK+, MUG, ISED, DISFA, OULU-VIS-Strong, FER2013 and micro: CASME-I, CASME-II, CAS(ME) $\hat{2}$, SAMM datasets.

5.5. Speed, Memory and Complexity analysis

The models generated through EmoNAS search are very lightweight and fast. Table 13 shows the memory, speed, and computational complexity of the models generated by EmoNAS in different macro and micro-expression datasets. The proposed models require trainable parameters of approximately ≈ 0.5 Million (M) except for FER2013 and CK+. This is substantially lower than MobileNet (3.2M), VGG16 (138M), VGG19 (144M) ResNet50 (31M). It is even lower than HiNet (1M) with much better accuracy over the same. Also, our models use less memory space (13-15MB) as compared to MobileNet (23.8 MB), VGG16 (500.3 MB), VGG19 (520.4 MB), and ResNet (88.4 MB). Hence, it can be useful for deployment in embedded devices. The speed over GPU shows that the proposed models are remarkably fast (up to 60 fps), which makes them suitable for real-time applications.

We further compare our work with the existing methods for both MER and FER in Table 14. The EmoNAS models require the lowest number of operations for inference with $\sim 0.55\sim 0.60$ million parameters in the model. Our model size is ~ 38 MB less than the existing NAS method (P-DARTS). Similarly, the total

Method	Pub-Year	Task	Size (mb)	Speed (fps)	Params (M)
Originet Verma et al. (2020b)	IJCNN-20	MER	14.3	~0.22	1.8
AffectiveNet Verma et al. (2020a)	Mult-20	MER	8.3	0.12	2.2
MobileNet Verma et al. (2019a)	LCS-19	MER	25.3	0.08	4.2
DARTS Liu et al. (2018b)	ICLR-19	MER	~16	~35	~0.9
P-DARTS Chen et al. (2019b)	ICCV-19	MER	52	~5	~3.6
EmoNAS	Ours	MER	~14	~35	~0.60
MobileNet Verma et al. (2019a)	LCS-19	FER	23.8	NA	3.2
HiNet Verma et al. (2019a)	LCS-19	FER	5.3	NA	1.0
DARTS Liu et al. (2018b)	ICLR-19	FER	17	~35	~1.0
P-DARTS Chen et al. (2019b)	ICCV-19	FER	51	~5	~3.5
DARTS Liu et al. (2018b)	ICLR-19	FER	~17	~35	~1.0
Auto-FERNet Li et al. (2021)	TNSE-21	FER	N/A	N/A	~2.1
ViT Kim et al. (2022)	Sensors-22	FER	N/A	N/A	~86.86
Squeeze ViT Kim et al. (2022)	Sensors-22	FER	N/A	N/A	~11.96
EmoNAS	Ours	FER	~14	~45	~0.55

Table 14: Comparative analysis of the complexity of the EmoNAS with existing methods.

number of parameters for EmoNAS is $6\times$ less than the P-DARTS. The inference speed in MER and FER is ~ 35 and ~ 45 , respectively. Moreover, our proposed EmoNAS is also more efficient as compared to recent vision transformer based FER models as shown in Table 14. Particularly, proposed EmoNAS is $155\times$ and $20\times$ less than the ViT and Squeeze viT Kim et al. (2022) FER models, respectively. Thus, the optimized networks discovered by EmoNAS are suitable for embedded devices used in real-time applications.

6. Conclusions

To the best of our knowledge, this paper presents the first attempt at a NAS-based approach for the task of FER in both macro and micro-level facial expressions. We proposed EmoNAS which is based on the optimization techniques presented in DARTS to expedite the searching process. The design decisions for EmoNAS are the result of careful analysis of the FER domain-specific challenges. The same is validated by its superior performance over DART and P-DART methods. The architecture search also led to the formulation of shal-

lower and lightweight CNNs. The resulting models achieve better performance compared to the existing state-of-the-art FER methods in 13 benchmark (7 FER and 6 MER) datasets. The searched models obtain higher accuracy with a fraction of the computational cost and very high inference speed. In the future, shared parameters-based schemes can be investigated in the search process to discover even better performance-aware architectures. Furthermore, the number of skip connections can be optimized separately for a better trade-off between complexity and performance. The decision of selecting the number of cells in evaluation could also be included as a parameter for optimization while searching. The proposed framework is designed to work with single image input. This requires pre-processing of the video data into a single instance feature map for MER analysis. In the future, we plan to design a framework to handle the image and raw video data input for both macro- and micro-expression problems.

References

- Aifanti, N., Papachristou, C., & Delopoulos, A. (2010). The mug facial expression database. In *11th International Workshop on Image Analysis for Multimedia Interactive Services WIAMIS 10* (pp. 1–4). IEEE.
- Ambadar, Z., Schooler, J. W., & Cohn, J. F. (2005). Deciphering the enigmatic face: The importance of facial dynamics in interpreting subtle facial expressions. *Psychological science*, *16*, 403–410.
- Aouayeb, M., Hamidouche, W., Soladie, C., Kpalma, K., & Segulier, R. (2021). Learning vision transformer with squeeze and excitation for facial expression recognition. *arXiv preprint arXiv:2107.03107*, .
- Baker, B., Gupta, O., Raskar, R., & Naik, N. (2017). Accelerating neural architecture search using performance prediction. *arXiv preprint arXiv:1705.10823*, .
- Bender, G., Kindermans, P.-J., Zoph, B., Vasudevan, V., & Le, Q. V. (2018). Understanding and simplifying one-shot architecture search. In *ICML*.

- Bilen, H., Fernando, B., Gavves, E., Vedaldi, A., & Gould, S. (2016). Dynamic image networks for action recognition. In *Proceedings of the IEEE Conference on Computer Vision and Pattern Recognition* (pp. 3034–3042).
- Cai, J., Meng, Z., Khan, A.-S., Li, Z., O’Reilly, J., & Tong, Y. (2019). Identity-free facial expression recognition using conditional generative adversarial network. *ArXiv, abs/1903.08051*.
- Chen, X., Xie, L., Wu, J., & Tian, Q. (2019a). Progressive differentiable architecture search: Bridging the depth gap between search and evaluation. In *Proceedings of the IEEE International Conference on Computer Vision* (pp. 1294–1303).
- Chen, X., Xie, L., Wu, J., & Tian, Q. (2019b). Progressive differentiable architecture search: Bridging the depth gap between search and evaluation. In *Proceedings of the IEEE International Conference on Computer Vision*, (pp. 1294–1303).
- Davison, A. K., Lansley, C., Costen, N., Tan, K., & Yap, M. H. (2016). Samm: A spontaneous micro-facial movement dataset. *IEEE Transactions on Affective Computing*, 9, 116–129.
- Ekman, P. (2003). Darwin, deception, and facial expression. *Annals of the New York Academy of Sciences*, 1000, 205–221.
- Ekman, P., & Friesen, W. V. (1971). Constants across cultures in the face and emotion. *Journal of personality and social psychology*, 17, 124.
- Fan, Y., Lam, J. C., & Li, V. O. (2018). Multi-region ensemble convolutional neural network for facial expression recognition. In *International Conference on Artificial Neural Networks* (pp. 84–94). Springer.
- Fan, Y., Li, V., & Lam, J. C. (2020). Facial expression recognition with deeply-supervised attention network. *IEEE Transactions on Affective Computing*,

- Gan, Y., Liong, S.-T., Yau, W.-C., Huang, Y.-C., & Tan, L.-K. (2019). Off-apexnet on micro-expression recognition system. *Signal Processing: Image Communication*, *74*, 129–139.
- Georgescu, M.-I., Ionescu, R. T., & Popescu, M. (2018). Local learning with deep and handcrafted features for facial expression recognition. *IEEE Access*, *7*, 64827–64836.
- Giannopoulos, P., Perikos, I., & Hatzilygeroudis, I. (2018). Deep learning approaches for facial emotion recognition: A case study on fer-2013. In *Advances in hybridization of intelligent methods* (pp. 1–16). Springer.
- Guoying, Z., & Pietikainen, M. (2007). Dynamic texture recognition using local binary patterns with an application to facial expressions. In *IEEE transactions on pattern analysis and machine intelligence* (pp. 915–928). volume 29.
- Happy, S. L., & Routray, A. (2017). Fuzzy histogram of optical flow orientations for micro-expression recognition. In *IEEE Transactions on Affective Computing*.
- He, K., Zhang, X., Ren, S., & Sun, J. (2015). Deep residual learning for image recognition. *2016 IEEE Conference on Computer Vision and Pattern Recognition (CVPR)*, (pp. 770–778).
- Howard, A. G., Zhu, M., Chen, B., Kalenichenko, D., Wang, W., Weyand, T., Andreetto, M., & Adam, H. (2017). Mobilenets: Efficient convolutional neural networks for mobile vision applications. *ArXiv, abs/1704.04861*.
- Ionescu, R. T., Popescu, M., & Grozea, C. (2013). Local learning to improve bag of visual words model for facial expression recognition. In *Workshop on challenges in representation learning, ICML*.
- Iqbal, M. T. B., Ryu, B., Ramirez Rivera, A., Makhmudkhujaev, F., Chae, O., & Bae, S. (2020). Facial expression recognition with active local shape pattern

- and learned-size block representations. *IEEE Transactions on Affective Computing*, (pp. 1–1). doi:10.1109/TAFFC.2020.2995432.
- Kaggle.com (2019 (accessed December 3, 2019)). *Challenges in Representation Learning: Facial Expression Recognition Challenge*. URL: <https://www.kaggle.com/c/challenges-in-representation-learning-facial-expression-recognition-challenge/>.
- Khor, H.-Q., See, J., Liong, S.-T., Phan, R. C., & Lin, W. (2019). Dual-stream shallow networks for facial micro-expression recognition. In *2019 IEEE International Conference on Image Processing (ICIP)* (pp. 36–40). IEEE.
- Khorrami, P., Paine, T. L., & Huang, T. S. (2015). Do deep neural networks learn facial action units when doing expression recognition? *2015 IEEE International Conference on Computer Vision Workshop (ICCVW)*, (pp. 19–27).
- Kim, D. H., Baddar, W. J., Jang, J., & Ro, Y. M. (2017). Multi-objective based spatio-temporal feature representation learning robust to expression intensity variations for facial expression recognition. In *IEEE Transactions on Affective Computing* (pp. 223–236). volume 10.
- Kim, S., Nam, J., & Ko, B. C. (2022). Facial expression recognition based on squeeze vision transformer. *Sensors*, *22*, 3729.
- Kuo, C.-M., Lai, S.-H., & Sarkis, M. (2018). A compact deep learning model for robust facial expression recognition. In *Proceedings of the IEEE conference on computer vision and pattern recognition workshops* (pp. 2121–2129).
- Li, J., Wang, Y., See, J., & Liu, W. (2019a). Micro-expression recognition based on 3d flow convolutional neural network. In *Pattern Analysis and Applications* (pp. 1331–1339). volume 22.
- Li, S., & Deng, W. (2020). Deep facial expression recognition: A survey. *IEEE Transactions on Affective Computing*, .

- Li, S., & Deng, W. (2020). A deeper look at facial expression dataset bias. *IEEE Transactions on Affective Computing*, (pp. 1–1). doi:10.1109/TAFFC.2020.2973158.
- Li, S., Deng, W., & Du, J. (2017). Reliable crowdsourcing and deep locality-preserving learning for expression recognition in the wild. In *Proceedings of the IEEE conference on computer vision and pattern recognition* (pp. 2852–2861).
- Li, S., Li, W., Wen, S., Shi, K., Yang, Y., Zhou, P., & Huang, T. (2021). Auto-ferret: A facial expression recognition network with architecture search. *IEEE Transactions on Network Science and Engineering*, 8, 2213–2222.
- Li, X., Pfister, T., Huang, X., Zhao, G., & Pietikäinen, M. (2013). A spontaneous micro-expression database: Inducement, collection and baseline. In *2013 10th IEEE International Conference and Workshops on Automatic face and gesture recognition (fg)* (pp. 1–6). IEEE.
- Li, Y., Huang, X., & Zhao, G. (2020a). Joint local and global information learning with single apex frame detection for micro-expression recognition. *IEEE Transactions on Image Processing*, 30, 249–263.
- Li, Y., Lu, G., Li, J., Zhang, Z., & Zhang, D. (2020b). Facial expression recognition in the wild using multi-level features and attention mechanisms. *IEEE Transactions on Affective Computing*, .
- Li, Y., Zeng, J., Shan, S., & Chen, X. (2019b). Occlusion aware facial expression recognition using cnn with attention mechanism. *IEEE Transactions on Image Processing*, 28, 2439–2450.
- Liong, S.-T., Gan, Y., See, J., Khor, H.-Q., & Huang, Y.-C. (2019a). Shallow triple stream three-dimensional cnn (ststnet) for micro-expression recognition. In *2019 14th IEEE International Conference on Automatic Face & Gesture Recognition (FG 2019)* (pp. 1–5). IEEE.

- Liong, S.-T., Gan, Y. S., John See, H.-Q. K., & Huang, Y.-C. (2019b). Shallow triple stream three-dimensional cnn (ststnet) for micro-expression recognition. In *In 2019 14th IEEE International Conference on Automatic Face & Gesture Recognition* (pp. 1–5). IEEE.
- Liu, C., Chen, L.-C., Schroff, F., Adam, H., Hua, W., Yuille, A. L., & Fei-Fei, L. (2019a). Auto-deeplab: Hierarchical neural architecture search for semantic image segmentation. In *Proceedings of the IEEE Conference on Computer Vision and Pattern Recognition* (pp. 82–92).
- Liu, C., Zoph, B., Neumann, M., Shlens, J., Hua, W., Li, L.-J., Fei-Fei, L., Yuille, A., Huang, J., & Murphy, K. (2018a). Progressive neural architecture search. In *Proceedings of the European Conference on Computer Vision (ECCV)* (pp. 19–34).
- Liu, H., Simonyan, K., & Yang, Y. (2018b). Darts: Differentiable architecture search. *arXiv preprint arXiv:1806.09055*, .
- Liu, K., Zhang, M., & Pan, Z. (2016). Facial expression recognition with cnn ensemble. *2016 International Conference on Cyberworlds (CW)*, (pp. 163–166).
- Liu, P., Han, S., Meng, Z., & Tong, Y. (2014). Facial expression recognition via a boosted deep belief network. *2014 IEEE Conference on Computer Vision and Pattern Recognition*, (pp. 1805–1812).
- Liu, Y., Du, H., Zheng, L., & Gedeon, T. (2019b). A neural micro-expression recognizer. In *2019 14th IEEE international conference on automatic face & gesture recognition (FG 2019)* (pp. 1–4). IEEE.
- Liu, Y.-J., Li, B.-J., , & Lai, Y.-K. (2018c). Sparse mdmo: Learning a discriminative feature for spontaneous micro-expression recognition. In *IEEE Transactions on Affective Computing*.
- Lopes, A. T., de Aguiar, E., de Souza, A. F., & Oliveira-Santos, T. (2017). Facial expression recognition with convolutional neural networks: Coping

with few data and the training sample order. *Pattern Recognition*, 61, 610–628.

- Lucey, P., Cohn, J. F., Kanade, T., Saragih, J., Ambadar, Z., & Matthews, I. (2010). The extended cohn-kanade dataset (ck+): A complete dataset for action unit and emotion-specified expression. In *2010 IEEE Computer Society Conference on Computer Vision and Pattern Recognition-Workshops* (pp. 94–101). IEEE.
- Mandal, M., Verma, M., Mathur, S., Vipparthi, S. K., Murala, S., & De-veerasetty, K. K. (2019). Regional adaptive affinitive patterns (radap) with logical operators for facial expression recognition. *IET Image Processing*, 13, 850–861.
- Mavadati, S. M., Mahoor, M. H., Bartlett, K., Trinh, P., & Cohn, J. F. (2013). Disfa: A spontaneous facial action intensity database. *IEEE Transactions on Affective Computing*, 4, 151–160.
- Mollahosseini, A., Chan, D., & Mahoor, M. H. (2016). Going deeper in facial expression recognition using deep neural networks. *2016 IEEE Winter Conference on Applications of Computer Vision (WACV)*, (pp. 1–10).
- Negrinho, R., & Gordon, G. (2017). Deeparchitect: Automatically designing and training deep architectures. *arXiv preprint arXiv:1704.08792*, .
- Pasupa, K., & Sunhem, W. (2016). A comparison between shallow and deep architecture classifiers on small dataset. In *2016 8th International Conference on Information Technology and Electrical Engineering (ICITEE)* (pp. 1–6). IEEE.
- Pons, G., & Masip, D. (2017). Supervised committee of convolutional neural networks in automated facial expression analysis. *IEEE Transactions on Affective Computing*, 9, 343–350.

- Qu, F., Wang, S.-J., Yan, W.-J., Li, H., Wu, S., & Fu, X. (2017). Cas(me)²: A database for spontaneous macro-expression and micro-expression spotting and recognition. *IEEE Transactions on Affective Computing*, 9, 424–436.
- Real, E., Aggarwal, A., Huang, Y., & Le, Q. V. (2019). Regularized evolution for image classifier architecture search. In *Proceedings of the aaai conference on artificial intelligence* (pp. 4780–4789). volume 33.
- Reddy Sai Prasanna Teja, Surya Teja Karri, Shiv Ram Dubey, & Snehasis Mukherjee (2019). Spontaneous facial micro-expression recognition using 3d spatiotemporal convolutional neural networks. In *In 2019 International Joint Conference on Neural Networks (IJCNN)* (pp. 1–8). IEEE.
- S. L. Happy, Priyadarshi Patnaik, Aurobinda Routray, & Rajlakshmi Guha (2017). The indian spontaneous expression database for emotion recognition. *IEEE Transactions on Affective Computing*, 8, 131–142.
- See, J., Yap, M. H., Li, J., Hong, X., & Wang, S.-J. (2019). Megc 2019—the second facial micro-expressions grand challenge. In *2019 14th IEEE International Conference on Automatic Face & Gesture Recognition (FG 2019)* (pp. 1–5). IEEE.
- Simonyan, K., & Zisserman, A. (2014). Very deep convolutional networks for large-scale image recognition. *CoRR*, *abs/1409.1556*.
- Song, B., Li, K., Zong, Y., Zhu, J., Zheng, W., Shi, J., & Zhao, L. (2019). Recognizing spontaneous micro-expression using a three-stream convolutional neural network. *IEEE Access*, 7, 184537–184551.
- Srivastava, R. K., Greff, K., & Schmidhuber, J. (2015). Training very deep networks. In *Advances in neural information processing systems* (pp. 2377–2385).
- Sun, B., Cao, S., Li, D., He, J., & Yu, L. (2020). Dynamic micro-expression recognition using knowledge distillation. *IEEE Transactions on Affective Computing*, (pp. 1–1). doi:10.1109/TAFFC.2020.2986962.

- Van Quang, N., Chun, J., & Tokuyama, T. (2019). Capsulenet for micro-expression recognition. In *2019 14th IEEE International Conference on Automatic Face & Gesture Recognition (FG 2019)* (pp. 1–7). IEEE.
- Verma, M., Reddy, M. S. K., Meedimale, Y. R., Mandal, M., & Vipparthi, S. K. (2021). Automer: Spatiotemporal neural architecture search for microexpression recognition. *IEEE Transactions on Neural Networks and Learning Systems*, .
- Verma, M., Vipparthi, S. K., & Singh, G. (2019a). Hinet: Hybrid inherited feature learning network for facial expression recognition. *IEEE Letters of the Computer Society*, *2*, 36–39.
- Verma, M., Vipparthi, S. K., & Singh, G. (2020a). Affectivenet: Affective-motion feature learning for micro expression recognition. *IEEE MultiMedia*, (pp. 1–1). doi:10.1109/MMUL.2020.3021659.
- Verma, M., Vipparthi, S. K., & Singh, G. (2020b). Non-linearities improve originet based on active imaging for micro expression recognition. In *2020 International Joint Conference on Neural Networks (IJCNN)* (pp. 1–8). doi:10.1109/IJCNN48605.2020.9207718.
- Verma, M., Vipparthi, S. K., Singh, G., & Murala, S. (2019b). Learnet: Dynamic imaging network for micro expression recognition. *IEEE Transactions on Image Processing*, *29*, 1618–1627.
- Wang, C., Peng, M., Bi, T., & Chen, T. (2018a). Micro-attention for micro-expression recognition. *arXiv preprint arXiv:1811.02360*, .
- Wang, C., Peng, M., Bi, T., & Chen, T. (2020a). Micro-attention for micro-expression recognition. *Neurocomputing*, *410*, 354–362.
- Wang, K., Peng, X., Yang, J., Lu, S., & Qiao, Y. (2020b). Suppressing uncertainties for large-scale facial expression recognition. In *Proceedings of the IEEE/CVF Conference on Computer Vision and Pattern Recognition (CVPR)*.

- Wang, S.-J., Li, B.-J., Liu, Y.-J., Yan, W.-J., Ou, X., Huang, X., Xu, F., & Fu, X. (2018b). Micro-expression recognition with small sample size by transferring long-term convolutional neural network. In *Neurocomputing* 312 (pp. 251–262).
- Wang, W., Sun, Q., Chen, T., Cao, C., Zheng, Z., Xu, G., Qiu, H., & Fu, Y. (2019). A fine-grained facial expression database for end-to-end multi-pose facial expression recognition. *ArXiv, abs/1907.10838*.
- Wen, Z., Lin, W., Wang, T., & Xu, G. (2021). Distract your attention: multi-head cross attention network for facial expression recognition. *arXiv preprint arXiv:2109.07270*, .
- Xia, Z., Liang, H., Hong, X., & Feng, X. (2019). Cross-database micro-expression recognition with deep convolutional networks. In *Proceedings of the 2019 3rd International Conference on Biometric Engineering and Applications* (pp. 56–60).
- Xia, Z., Peng, W., Khor, H.-Q., Feng, X., & Zhao, G. (2020). Revealing the invisible with model and data shrinking for composite-database micro-expression recognition. *IEEE Transactions on Image Processing*, 29, 8590–8605.
- Xie, S., & Hu, H. (2019). Facial expression recognition using hierarchical features with deep comprehensive multipatches aggregation convolutional neural networks. *IEEE Transactions on Multimedia*, 21, 211–220.
- Xie, Y., Chen, T., Pu, T., Wu, H., & Lin, L. (2020). Adversarial graph representation adaptation for cross-domain facial expression recognition. In *Proceedings of the 28th ACM international conference on Multimedia* (pp. 1255–1264).
- Xu, F., Zhang, J., , & Wang, J. Z. (2017). Microexpression identification and categorization using a facial dynamics map. In *IEEE Transactions on Affective Computing* (pp. 254–267). volume 8.

- Yan, W.-J., Li, X., Wang, S.-J., Zhao, G., Liu, Y.-J., Chen, Y.-H., & Fu, X. (2014). Casme ii: An improved spontaneous micro-expression database and the baseline evaluation. *PloS one*, *9*, e86041.
- Yan, W.-J., Wu, Q., Liu, Y.-J., Wang, S.-J., & Fu, X. (2013). Casme database: a dataset of spontaneous micro-expressions collected from neutralized faces. In *2013 10th IEEE international conference and workshops on automatic face and gesture recognition (FG)* (pp. 1–7). IEEE.
- Yang, B., Cheng, J., Yang, Y., Zhang, B., & Li, J. (2021). Merta: micro-expression recognition with ternary attentions. *Multimedia Tools and Applications*, *80*, 1–16.
- Yang, H., Zhang, Z., & Yin, L. (2018). Identity-adaptive facial expression recognition through expression regeneration using conditional generative adversarial networks. *2018 13th IEEE International Conference on Automatic Face & Gesture Recognition (FG 2018)*, (pp. 294–301).
- Yong-Jin, L., Jin-Kai, Z., Wen-Jing, Y., Su-Jing, W., Guoying, Z., & Xiaolan, F. (2015). A main directional mean optical flow feature for spontaneous micro-expression recognition. *IEEE Transactions on Affective Computing*, *7*, 299–310.
- Yu, Z., Qin, Y., Xu, X., Zhao, C., Wang, Z., Lei, Z., & Zhao, G. (2020a). Auto-fas: Searching lightweight networks for face anti-spoofing. In *ICASSP 2020-2020 IEEE International Conference on Acoustics, Speech and Signal Processing (ICASSP)* (pp. 996–1000). IEEE.
- Yu, Z., Wan, J., Qin, Y., Li, X., Li, S. Z., & Zhao, G. (2020b). Nas-fas: Static-dynamic central difference network search for face anti-spoofing. *arXiv preprint arXiv:2011.02062*, .
- Yu, Z., Zhao, C., Wang, Z., Qin, Y., Su, Z., Li, X., Zhou, F., & Zhao, G. (2020c). Searching central difference convolutional networks for face anti-

- spoofing. In *Proceedings of the IEEE/CVF Conference on Computer Vision and Pattern Recognition* (pp. 5295–5305).
- Zhang, T., Zheng, W., Cui, Z., Zong, Y., Yan, J., & Yan, K. (2016). A deep neural network-driven feature learning method for multi-view facial expression recognition. *IEEE Transactions on Multimedia*, *18*, 2528–2536.
- Zhang, T., Zong, Y., Zheng, W., Chen, C. L. P., Hong, X., Tang, C., Cui, Z., & Zhao, G. (2020). Cross-database micro-expression recognition: A benchmark. *IEEE Transactions on Knowledge and Data Engineering*, (pp. 1–1). doi:10.1109/TKDE.2020.2985365.
- Zhao, G., Huang, X., Taini, M., Li, S. Z., & Pietikäinen, M. (2011). Facial expression recognition from near-infrared videos. *Image and Vision Computing*, *29*, 607–619.
- Zhao, S., Cai, H., Liu, H., Zhang, J., & Chen, S. (2018). Feature selection mechanism in cnns for facial expression recognition. In *BMVC* (p. 317).
- Zheng, C., Mendieta, M., & Chen, C. (2022). Poster: A pyramid cross-fusion transformer network for facial expression recognition. *arXiv preprint arXiv:2204.04083*, .
- Zhou, L., Mao, Q., & Xue, L. (2019). Dual-inception network for cross-database micro-expression recognition. In *2019 14th IEEE International Conference on Automatic Face & Gesture Recognition (FG 2019)* (pp. 1–5). IEEE.
- Zhou, L., Shao, X., & Mao, Q. (2020). A survey of micro-expression recognition. *Image and Vision Computing*, (p. 104043).
- Zoph, B., Vasudevan, V., Shlens, J., & Le, Q. V. (2018). Learning transferable architectures for scalable image recognition. In *Proceedings of the IEEE conference on computer vision and pattern recognition* (pp. 8697–8710).